

Fast and Efficient Epoxidation of Olefins Catalyzed by Brominated Mn(III) Salophen Grafted onto CoFe₂O₃/Graphene Oxide as a Heterogeneous Catalyst

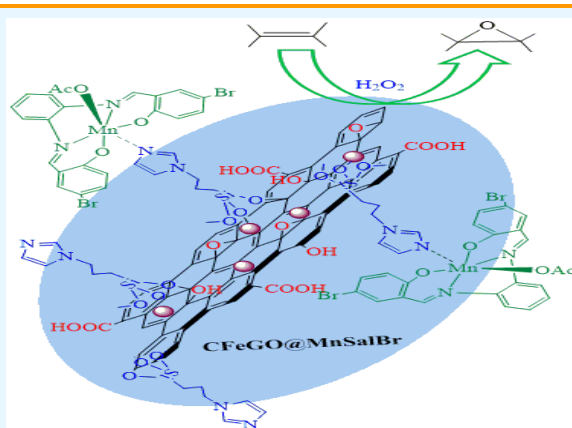
Robabeh Hajian*

Department of Chemistry, Yazd University, Yazd 89195-741, Iran

Received: November 4, 2021; Accepted: December 17, 2021

Cite This: *Inorg. Chem. Res.* **2022**, *6*, 1-9. DOI: 10.22036/icr.2021.312540.1120

Abstract: This study aims to prepare di-brominated Mn(III) Salophen, [MnSalBr], grafted onto CoFe₂O₃/graphene oxide (CFGO) via a covalent bond. The characterization of this heterogeneous catalyst (CFE@MnSalBr) was carried out by FTIR, DR UV-Vis, XRD, FESEM, EDX spectroscopy, elemental scanning mappings, thermogravimetric analysis (TGA/DTG), and nitrogen adsorption-desorption isotherm. The amount of manganese salophen loading on the CFG support was determined by inductively coupled plasma spectroscopy (ICP). At room temperature, the as-prepared catalyst was applied to oxidize olefins with H₂O₂ as a green oxidant. The result confirmed this catalyst's high catalytic reactivity and excellent selectivity in the epoxidation of various alkenes. The effects of different factors such as the kind of solvent and oxidant, amount of catalyst and oxidant, and reaction time were also studied. Furthermore, the GO-bound Mn salophen was reused for several runs without any noticeable activity loss or selectivity.



Keywords: Graphene oxide, Epoxidation, Heterogeneous catalyst, H₂O₂, Mn-salophen

1. INTRODUCTION

Epoxides serve as important precursors for synthesizing various chemical and industrial products. In this regard, epoxidation of olefins has attracted great attention.¹⁻³ Among the various single-oxygen donors for epoxidation, H₂O₂ is an eco-friendly, affordable, and highly available oxidant, with water as a by-product.⁴ Schiff bases or imines can be synthesized by condensing aldehydes or ketones and primary amines. Schiff base complexes have found a range of applications in polymerizing different monomers,⁵ oxidation reactions,⁶⁻⁸ and biological fields.⁹ The curious thing about Schiff base complexes is the preparation of salen and salophen compounds. Manganese salen/salophen is known as a powerful catalyst for the oxidation of various organic composites.^{4,10-13} In addition, Mn-salophen has been discovered in active sites of many enzymes.¹⁴ Due to the ease of product separation, reusability, high stability, and adaptability to green chemistry, heterogeneous catalysts are desirable to use. Over the past two decades, the immobilization of homogenous catalysts on appropriate supports has become a consequential field in synthesizing valuable materials. To this end, various organic and inorganic supports with excellent surface areas have been used to

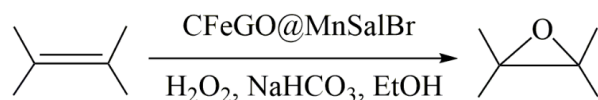
heterogenized homogenous catalysts efficiently. Some of these supports are polymers,^{15,16} mesoporous silica,^{10,17-19} inorganic nanoparticles,²⁰ zeolite²¹ and carbon nanotubes.^{13,22,23} Heterogenization occurs via electrostatic, encapsulation, adsorption binding, covalent attachment, and axial coordination onto or in many supports.²⁴ The supported Schiff base complexes of salophen have exhibited significant catalytic activity in various inorganic reactions.²⁵⁻²⁸

Over the last decades, graphene oxide (GO) has been widely used due to its unique and novel nanostructure, high specific surface area, vast chemical stability, and good accessibility.^{29, 30}

Numerous oxygen-containing functional groups (including -COOH, -OH, and epoxy groups) on both basal planes and sheet edges can be readily functionalized and modified into a wide range of materials.^{31,32} Some publications have reported the use of GO-supported metal Schiff base complexes, such as copper,^{8,33-37} vanadium,^{38,39} cobalt,⁴⁰ molybdenum,⁴¹ and manganese.^{42,43} However, these catalytic materials still have some limitations in that they cannot be easily separated from reaction mixtures. Using magnetic nanoparticles (MNPs) is an excellent solution to this problem as they can be easily retrieved from reaction systems with a magnet.

Spinel ferrite, as a specific family member of MNPs with the general formula of MFe_2O_3 (M: Mn, Fe, Co, Cu, and Ni), has attracted much attention due to its good properties, such as low toxicity, environmental friendliness, high ratio of surface area to volume and superparamagnetic behavior.⁴⁴ This material is a crystalline composite applied to electronic devices, magnetic materials, ceramic glaze, and biomedical products.⁴⁵⁻⁴⁸ Also, spinel cobalt ferrite ($CoFe_2O_4$) is a special magnetic-core carrier that is easier to prepare than Fe_3O_4 and does not require the use of a nitrogen environment.^{49,50} There are many reports in the literature on the design and catalytic performance of ferrite-supported Schiff base complexes.⁵¹⁻⁵³ A combination of ferrite nanoparticles and graphene oxide as supports synergistically gains the advantages of both substances. Despite $CoFe_2O_4/GO$ having been previously reported in other reactions as a catalyst,^{54,55} there is no report on the use of $CoFe_2O_4/GO$ hybrids as a catalytic epoxidation. Furthermore, such hybrids can be used for grafting functional groups onto surfaces and improving the specific surface. That makes it a good candidate to support. Very few studies deal with magnetite graphene oxide-immobilized Schiff bases as heterogeneous catalysts. For example, Abbasi and colleagues prepared Mn-Schiff base complexes on Fe_3O_4 /graphene oxide sheets to oxidize olefins.^{56,57}

In line with the research on developing heterogeneous catalysts for oxidation reactions,⁸⁻⁶² the present study synthesized a new heterogeneous catalyst by anchoring di-brominated manganese salophen on $CoFe_2O_4$ /graphene oxide-bound imidazole (CFGO) through a covalent bond. Imidazole was selected because they bind strongly to the axial positions of metalosalophen in solution,^{63,64} and such nitrogen bases can enhance catalytic activity in the epoxidation with single oxygen atom donors. The prepared catalyst was then used to oxidate various olefins in the presence of H_2O_2 and $NaHCO_3$ as co-catalysts under mild conditions (Scheme 1). The observations indicated that $CFGO@MnSalBr$ could not only serve as a highly efficient catalyst for the epoxidation of olefins but also has excellent stability even after several runs. This catalyst was easily recoverable from reaction mixtures with an external magnet.



Scheme 1. Oxidation of alkenes with H_2O_2 catalyzed by $CFEGO@MnSalBr$

2. EXPERIMENTAL

Materials and methods

All the chemicals were of analytical grades and used as received. Fourier transform infrared spectra were taken with a Bruker FT-

IR Equinox-55 spectrophotometer in the range of 400-4000 cm^{-1} as KBr disks. Diffuse reflectance UV-Vis spectra were plotted on a Jasco V-670 spectrometer. Powder X-ray diffraction (XRD) data were recorded on a D₈ Advanced Bruker using Cu-K α radiation. The FESEM images were taken, and energy-dispersive X-ray spectroscopy (EDX) analyses were performed using a TE-SCAN MIRA (Czech) instrument. A thermogravimetric analysis (TGA) was conducted on STD Q600 in N_2 atmosphere at a heating rate of 10 $^{\circ}C\ min^{-1}$. The ICP analyses were performed on an ICP-Spectrociros CCD instrument. The BET surface area, the nitrogen adsorption-desorption isotherm, volume, pore diameter, and the other surface properties of the compounds were obtained by a BELSORB-mini II. The catalysis results were analyzed using an Agilent 7890N gas chromatograph equipped with 19091J-413 HP-5 capillary column and a flame ionization detector with n-decane as the internal standard.

Preparation of catalysts

Functionalization of $GO.Cl$ nanoparticles with imidazole, $GO.Im$

Graphene oxide was prepared and purified by an improved Hummers process.⁶⁵ A mixture of GO (1 g) and toluene (30 mL) was ultrasonically dispersed for half an hour, and then 1.8 mL of 3-chloropropyltrimethoxysilane (10 mmol) was added under nitrogen protection through a procedure reported previously.³⁶ In the next step, the prepared chloropropylated GO ($GO.Cl$) nanoparticles and 60 mL of acetonitrile were subjected to ultrasonic treatment for 20 min, and then imidazole (10 mmol) was added. After the solution was stirred under reflux for 48 h, the product ($GO.Im$) was filtered, washed three times with 10 mL of CH_3CN , and then dried overnight under vacuum at 80 $^{\circ}C$.

Preparation of a magnetite support $CoFe_2O_4/GO.Im$ (CFGO)

Cobalt ferrite $CoFe_2O_4$ nanoparticles were obtained via the coprecipitation procedure based on the method reported in the literature.⁶⁶ To prepare the magnetite support graphene oxide (CFGO), a solution of $GO.Im$ (15 mg) ultrasonically dispersed in 30 mL of deionized water was added dropwise to 15 mg of a $CoFe_2O_4$ suspension in deionized water. The mixture was kept under vigorous stirring at 80 $^{\circ}C$ for an hour. The black precipitate was separated with a strong external magnet, washed several times with deionized water and ethanol, and dried in a vacuum.

Immobilization of Mn(III) Salophen [$MnSalBr$] on $CoFe_2O_4/GO.Im$ nanoparticles ($CFEGO@MnSalBr$)

To prepare di-brominated Mn(III) Salophen [$MnSalBr$], first, a solution of benzene-1,2-diamine (25 mmol) in 30 mL of EtOH was added to a solution of 5-bromo-2-hydroxybenzaldehyde (50 mmol) in EtOH. The resulting mixture was stirred at room temperature for 30 min. Then, 30 mL of an ethanolic solution of $Mn(CH_3COOH)_2 \cdot 4H_2O$ (10 mmol) was added dropwise to the stirred mixture, and the new solution was stirred for 3 h. The product was centrifuged and washed several times with EtOH and dried under vacuum at room temperature several times.⁶⁷ Next, 3 g of the CFGO support was dispersed in 100 mL of toluene for half an h. Also, 0.5 g of [$MnSalBr$] was added to this

mixture. The resulting mixture was stirred at 80 °C for 48 h. The product was collected using a permanent magnet, washed with methanol and ether, and dried at 60 °C overnight. The Mn-salophen loading on the CFeGO@MnSalBr catalyst was evaluated by measuring manganese through inductively coupled plasma (ICP).

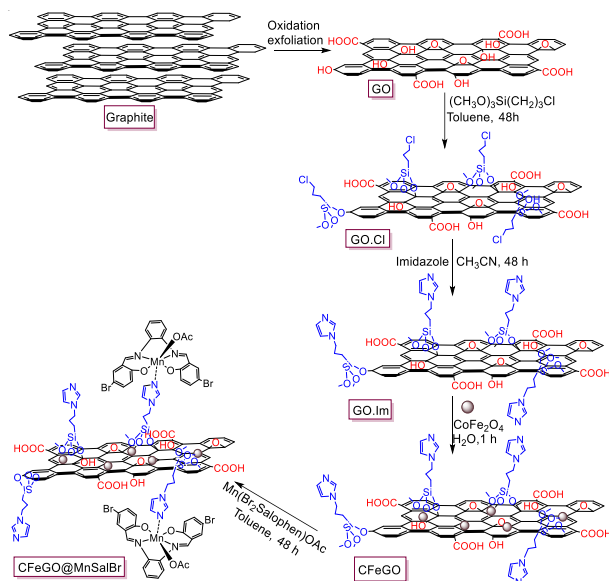
Catalytic activity and stability of CFeGO@MnSalBr

Typically, 0.5 mL of hydrogen peroxide as a green oxidant was added to a mixture of olefin (0.5 mmol) and CFeGO@MnSalBr (100 mg) in EtOH (4 mL) and NaHCO₃ as a co-catalyst (0.5 mmol). The mixture was kept under stirring at room temperature for several minutes. The products and the unconverted reactants were monitored using GC with n-decane as the internal standard. After the completion of the reaction, the organic compounds were extracted with diethyl ether and purified with silica gel. In the recycling experiments, the desired catalyst was separated with an external magnet, washed with Et₂O twice, and then dried carefully.

3. RESULTS AND DISCUSSION

Characterization of the catalyst (CFeGO@MnSalBr)

Scheme 2 displays the procedure for the preparation of GO and the covalent bonding of Mn-salophen to GO through imidazole groups (CFeGO@MnSalBr). This new catalyst was characterized by FT-IR, DR UV-Vis, XRD, FESEM, EDX, TGA/DTG, ICP, and nitrogen adsorption-desorption isotherm. The amount of MnSalBr supported on the GO and measured by ICP was 0.3 mmol g⁻¹ based on manganese.



Scheme 2. The schematic diagram for the preparation of CFeGO@MnSalBr

The DR UV-Vis spectra of CFeGO and CFeGO@MnSalBr catalysts are presented in Figure 1.

The CFeGO has several bands at 215, 251, 309, 326, and 395 nm, attributed to the ligand-to-metal charge transfer of CoFe₂O₄. After loading manganese salophen onto CFeGO, the absorption bands can be seen at 275 (n-π* transition of the azomethine chromophore), 385 nm (MLCT of Mn(III) salophen complex).⁸ This result indicates the presence of the manganese catalyst on the CFeGO support.

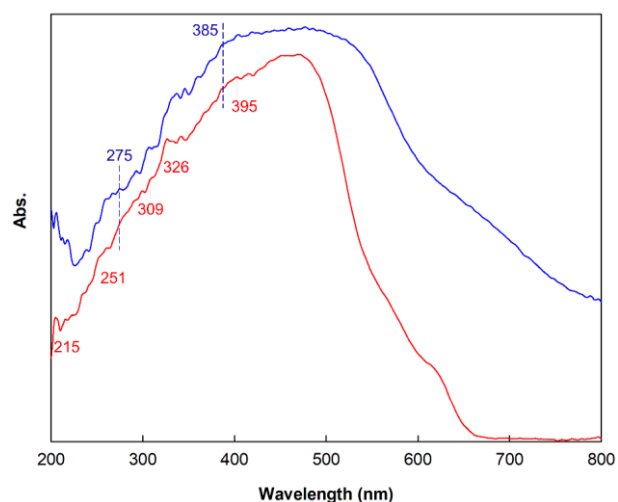


Figure 1. DR UV-Vis spectra of (a) CFeGO and (b) CFeGO@MnSalBr.

Figure 2 shows the FT-IR spectra of GO, GO.Cl, GO.Im, manganese salophen, and Mn salophen supported on the (CoFe₂O₄/GO.Im) surface. The stretching vibrations of C=O (carboxyl), C=C (aromatic ring), C-OH (hydroxyl groups), and C-O (epoxy) at 1733, 1623, 1226, and 1049 cm⁻¹, respectively, can be seen in the IR spectrum of solid GO (Figure 2a).⁴² The strong peaks at 999 and 1120 cm⁻¹ can be assigned to Si-O-C and Si-O-Si, representing the successful silylation of graphene oxide nanosheets through chemical bonding (Figure 2b).³⁵ After imidazole was grafted to GO.Cl, the bands at 1442 and 1509 cm⁻¹ were associated with the stretching vibrations of C-N and C=N of the imidazole group (Figure 2c).¹⁶ In Figure 2d, the peak at 1607 belongs to the stretching vibration of C=N of the imine group in the Schiff base units. Furthermore, the bands at 1450-1650 cm⁻¹ can be attributed to the stretching vibrations of C=C bonds of the phenyl ring. The bands at 1395 cm⁻¹ are attributed to the acetate ions (OAc) for this complex. The FT-IR spectra of CFeGO@MnSalBr and the recovered CFeGO@MnSalBr are depicted in Figures 2e and 2f. The emergence of broadband at about 574 cm⁻¹ and 449 cm⁻¹ is due to the presence of the Co(II)-O²⁻ (octahedral sites) and Fe(III)-O²⁻ (tetrahedral sites) bond of the spinel cobalt ferrite phase, respectively.⁶⁸ The FTIR spectrum of CFeGO@MnSalBr exhibits a strong peak at 1600 cm⁻¹ in the C=N stretch belonging to the characteristic peaks of the Mn salophen complex. Moreover, the peaks at 1017

and 1121 cm^{-1} demonstrate the presence of silanol groups, and the bonds at 1449 cm^{-1} reveal imidazole groups (Figure 2e). These observations prove that manganese salophen was successfully immobilized on the ($\text{CoFe}_2\text{O}_4/\text{GO.Im}$) support.

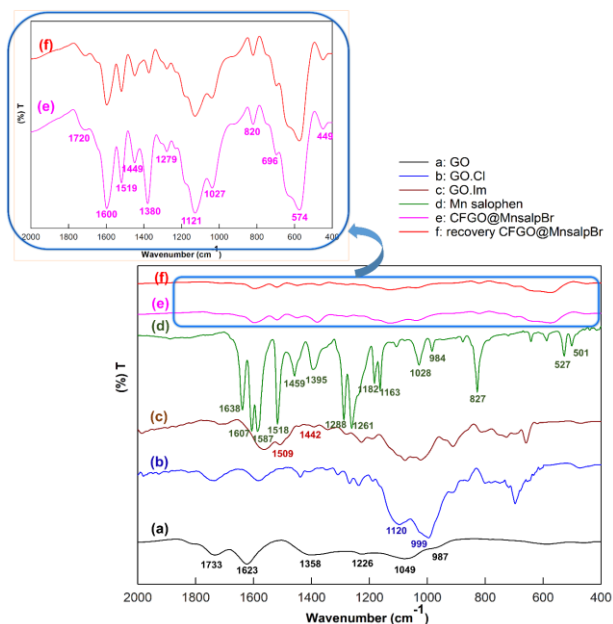


Figure 2. FT-IR spectra of (a) GO, (b) GO.Cl, (c) GO.Im, (d) MnSalphen, (e) CFGeO@MnSalBr and (f) recovered CFGeO@MnSalBr.

To characterize the crystalline structures of $\text{CoFe}_2\text{O}_4\text{-GO}$ (CFGeO) and CFGeO@MnSalBr, their XRD patterns were obtained, as exhibited in Figure 3. The diffraction peaks at (111), (220), (311), (400), (422), (511), and (440) matched the planes of the face-centered cubic CoFe_2O_4 nanoparticles (JCPDS Card no. 22-1076).⁶⁹ There were no diffraction peaks for the GO sheets in CFGeO, which can be attributed to the strong signals of the cobalt ferrite spinel tending to overwhelm the weak graphene oxide peak ($2\theta = 11\text{-}12$) or due to the low content of GO in CFGeO (Figure 3a).⁵⁷ Upon the immobilization of the Mn salophen complex on CFGeO, the typical XRD peaks became weak and broad compared to CFGeO, which proves the successful preparation of the CFGeO@MnSalBr compound (Figure 3b).

The FTSEM image and the size distribution histogram of the heterogeneous catalyst are shown in Figures 4a and 4b. The FESEM image of CFGeO@MnSalBr shows an agglomerated layered structure that incorporates Mn(salophen) moieties between the magnetite GO nanosheets (Figure 4a). The size distribution for this specimen is about 61 nm, with particle sizes ranging from 20 to 120 nm (Figure 4b). The elemental mapping of the selected regions in the catalyst texture was also performed to understand the distribution of the heterogeneous catalyst (MnSalBr) on the CFGeO support. Figure 4 (c-k)

depicts the distribution of chloride, nitrogen, manganese, carbon, bromide, iron, silicon, and oxygen. In addition, according to the energy-dispersive X-ray spectroscopy (EDX) of CFGeO@MnSalBr, Mn and Br peaks originated from Mn salophen, demonstrating the attachment of the catalyst to the cobalt ferrite-GO (Figure 4l).

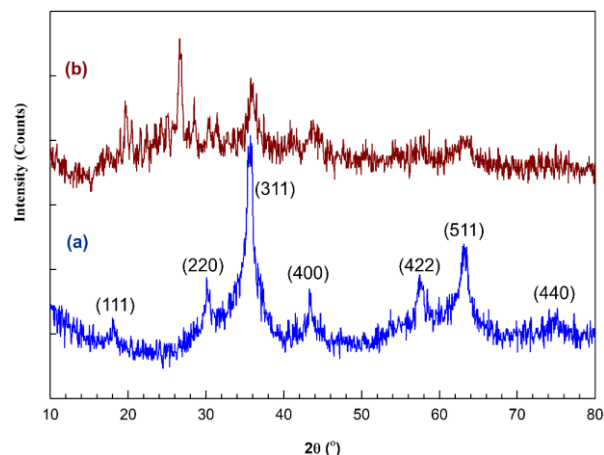


Figure 3. XRD patterns of (a) CFGeO and (b) CFGeO@MnSalBr.

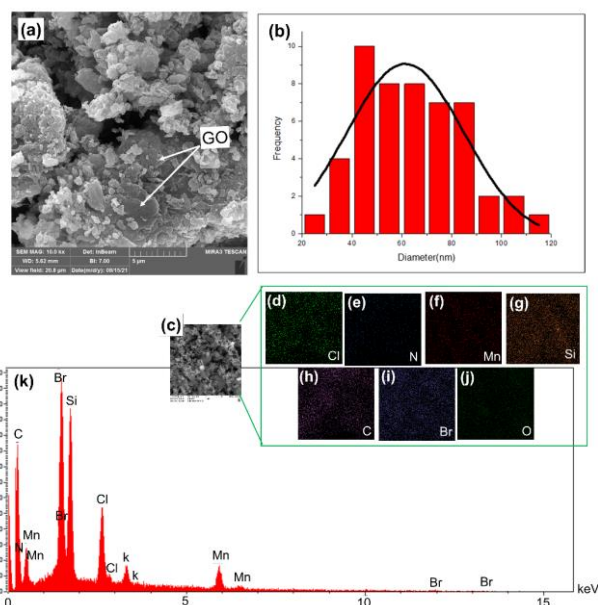


Figure 4. (a) FE-SEM image of CFGeO@MnSalBr, (b) histogram of the particle size of CFGeO@MnSalBr, (c-j) elemental mapping image of the sample separated once, and (k) EDX spectrum of CFGeO@MnSalBr

The thermogravimetric analysis (TGA) of CFGeO@MnSalBr yielded a pattern presented in Figure 5. According to the literature, graphene oxide is thermally unstable. It shows two distinct weight loss steps in the range of $20\text{-}700^\circ\text{C}$ that belong to the loss of the physically adsorbed water and the pyrolysis of oxygen-carrying functional groups.⁸ The TG cure of CFGeO@MnSalBr also shows two significant weight

losses in the temperature range of 35-750 °C. A low weight loss (5 wt%) below 100 °C occurred due to the elimination of the water physically adsorbed on the catalyst surface. The second significant weight loss in the range of 270-550 °C can be attributed to the thermal decomposition of the Mn salophen (about 70%). Remarkably, this catalyst system maintained its high stability below 270 °C, indicating the applicability of CFeGO@MnSalBr in epoxidation reactions.

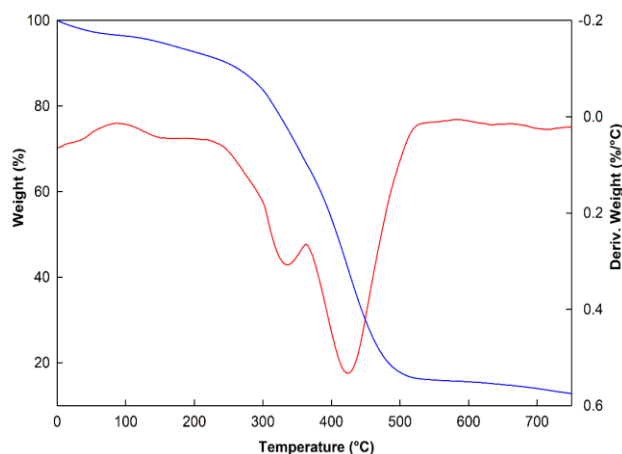


Figure 5. TGA curve for CFeGO@MnSalBr.

The N_2 adsorption-desorption isotherm of CFeGO@MnSalBr is presented in Figure 6. According to the IUPAC classification, the isotherm is type IV, characteristic of mesoporous solids. The BET surface area and the mean pore diameter of the catalyst were $16.27 \text{ m}^2 \text{ g}^{-1}$ and 52 nm, respectively. In addition, the BJH cumulative pore volume of CFeGO@MnSalBr was $0.2014 \text{ cm}^3 \text{ g}^{-1}$.

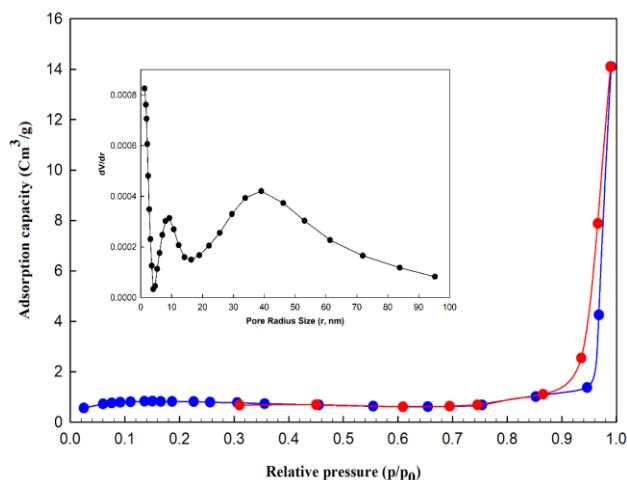


Figure 6. N_2 adsorption isotherms and pore distribution of CFeGO@MnSalBr.

Catalytic performance

The catalytic performance of CFeGO@MnSalBr in a heterogenized form was investigated for the epoxidation of cis-cyclooctene with H_2O_2 as an oxidant at room temperature. For this purpose, the effects of different parameters such as the amount of the catalyst, solvent type, and oxidant's kind were examined in detail (Table 1). First, the effect of the catalyst dosage on the oxidation of cyclooctene was investigated (Table 1: entry 1-4). Remarkably, in the absence of the catalyst, only 7% of the cyclooctene oxide was observed even after a prolonged reaction time. As the results suggested, the conversion of cyclooctene increased as the quantities of the catalyst rose from 25 mg to 100 mg. Also, a higher catalyst dosage had no noticeable effect on the reaction conversion. Hence, 100 mg (0.03 mmol) of the heterogeneous catalyst was applied in each experiment. Various solvents were tested in epoxidation reactions (Table 1: entry 5-11) to choose the reaction media. Although the best result was achieved in the mixture of acetonitrile, EtOH was selected as the most appropriate solvent for the oxidation of alkenes due to being eco-friendly and non-halogenated. Another fundamental factor in the oxidation of olefins is the nature of the oxygen donor. The effects of several oxidants such as $NaIO_4$, H_2O_2 , tert-BuOOH, Oxone ($KHSO_5$), and UHP (urea- H_2O_2) were studied in the oxidation of the cyclooctene catalyzed by CFeGO@MnSalBr. The data in Table 1 (entry 11-18) show that H_2O_2 is the best source of oxygen due to its good oxidation conversion and being a green oxidant. The effect of $NaHCO_3$ as a co-catalyst on the catalytic performance of the CFeGO@MnSalBr/ H_2O_2 system was noticeable. Research also indicates that bicarbonate is a suitable activator of H_2O_2 in the oxidation of alkenes by forming HCO_4^- ions.^{70, 71} The present study result also revealed that the highest catalytic activity could be achieved with the molar ratio of 1:10:1 for alkene: H_2O_2 : $NaHCO_3$. As an activator of H_2O_2 , sodium bicarbonate, is essential for the rate of oxidation reactions. Figure 7 presents the time courses of GO, CFeGO, MnSalBr, and CFeGO@MnSalBr under similar reaction conditions. The supporting solid GO and CFeGO did not represent a notable catalytic performance. The immobilization of Mn-salophen on CFeGO led to an increase in the conversion that occurred through the epoxidation reaction. The higher conversion of CFeGO@MnSalBr compared to the homogeneous system (MnSalBr) can be attributed to the high tendency of MnSalBr for aggregation and the isolation of the active system site of the graphene oxide solid.

The catalytic performance of CFeGO@MnSalBr was studied for the oxidation of various olefins (i.e., cyclic, phenyl-substituted, and linear) to the corresponding epoxides in EtOH. In this study, H_2O_2 was used as an oxidant under optimized conditions.

Table 1. The influence of the reaction conditions on the oxidation of cyclooctene catalyzed by CFeGO@MnSalBr: Influence of the catalyst amount (entry 1-4), Influence of the type of solvent (entry 5-10) and Influence of the type of oxidant (entry 11-18) on the oxidation of cyclooctene catalyzed by CFeGO@MnSalBr after 10 min^a

Entry	Catalyst (mmol)	Oxidant type	NaHCO ₃ (mmol)	Solvent type	Conversion (%) ^b
1	0	H ₂ O ₂	0.5	EtOH	7
2	0.015	H ₂ O ₂	0.5	EtOH	73
3	0.03	H ₂ O ₂	0.5	EtOH	98
4	0.06	H ₂ O ₂	0.5	EtOH	98
5	0.03	H ₂ O ₂	0.5	CH ₃ CN	100
6	0.03	H ₂ O ₂	0.5	EtOH	98
7	0.03	H ₂ O ₂	0.5	MeOH	87
8	0.03	H ₂ O ₂	0.5	CH ₂ Cl ₂	56
9	0.03	H ₂ O ₂	0.5	Acetone	46
10	0.03	H ₂ O ₂	0.5	CH ₃ Cl	42
11	0.03	Oxon	-	EtOH	29
12	0.03	t-BuOOH	-	EtOH	41
13	0.03	UHP	-	EtOH	38
14	0.03	NaIO ₄	-	EtOH	26
15	0.03	H ₂ O ₂	-	EtOH	67
16	0.03	H ₂ O ₂ [*]	0.5	EtOH	73
17	0.03	H ₂ O ₂ ^{**}	0.5	EtOH	98
18	0.03	H ₂ O ₂ ^{***}	0.5	EtOH	96

^aReaction conditions: cyclooctene (0.5 mmol), solvent (4 mL). ^bGC yield based on the starting cyclooctene. ^{*}(0.25 mmol), ^{**}(0.5 mmol), ^{***}(0.75 mmol).

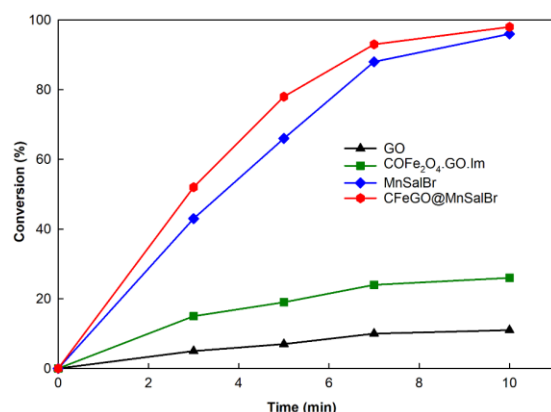


Figure 7. Conversion-time curves for the oxidation of cyclooctene with GO, CFeGO, MnSalBr, and CFeGO@MnSalBr. Reaction conditions: The molar ratios for Alkene: H₂O₂:NaHCO₃ are (1:10:1) with 100 mg of GO, CFeGO, MnSalBr, CFeGO@MnSalBr, and the molar ratios for MnSalBr: Alkene: H₂O₂:NaHCO₃ are (2:33:330:33); EtOH (4 mL).

The oxidation reactions were monitored by GC analysis until no further progress was observed. To calculate the longevity of this catalytic system, the total turnover frequency (TOF) was studied (see Table 2). In the heterogeneous catalytic system, cis-cyclooctene was a suitable substrate with 98% conversion and 100% epoxide selectivity. In the epoxidation of cyclohexene, cyclohexene oxide was the primary product (92%), and only trace amounts of the allylic oxidation products (i.e., cyclohexene-1-one and cyclohexene-1-ol) were produced. Styrene was transformed into styrene epoxide with 85% conversion, and only a small amount of benzaldehyde was obtained as a by-product. In comparison, α -methyl styrene showed slightly high activity with 90% conversion. The higher electron density in the double bond may have accounted for more epoxidation reactivity. In the case of α -methyl styrene, acetophenone was produced as a minor product. The oxidation of limonene was carried out with 70%

conversion and 100% epoxide selectivity (88% of 1,2-epoxide and 12% of 8,9-epoxide). In the case of α -pinene, a desired amount of epoxide was obtained (93%), and only trace amounts of verbenone and verbenol were produced. Indene was converted to its corresponding epoxide (71%) with 100% selectivity. The results also indicated that linear olefins with terminal double bonds, i.e., 1-hexene and 1-octene, had lower reactivity for oxidation than cyclic homolog due to increased steric hindrance. The oxidation of 1-hexene and 1-octene into the corresponding epoxides was carried out entirely with 43% and 32% conversion rates respectively.

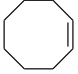
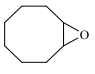
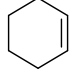
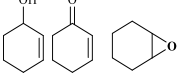
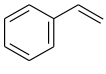
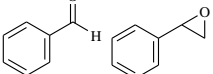
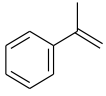
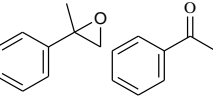
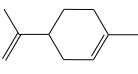
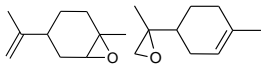
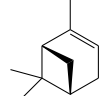
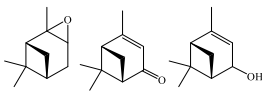
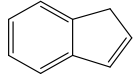
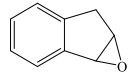
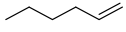
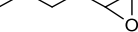
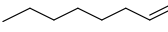

To show the effectiveness of the prepared catalyst, the turnover frequency of the catalytic system of CFeGO@MnSalBr for the epoxidation of cyclooctene, cyclohexene, and styrene was compared with that of the previously reported system of the supported manganese salophen (Table 3). The results could be due to the dispersion of the catalyst on graphene oxide, the separation of the active catalytic sites, thus, increased catalytic activity.

A possible mechanism for the Mn(III)-Salophen-mediated oxidation of olefins with H₂O₂/NaHCO₃ is the formation of manganese-acyl peroxydicarbonate species or a high-valent Mn=O intermediate in the catalytic process⁷¹.

Catalyst reuse and stability

The recovery and reusability of CFeGO@MnSalBr as a heterogeneous catalyst was studied using cis-cyclooctene as a model substrate. At the end of each reaction, the catalyst was easily separated with an external magnet (Figure 8), washed with EtOH twice, and then dried before use in the subsequent run. The filtrates were used to determine the amount of manganese leached by atomic absorption spectroscopy (AAS). The amount of Mn in the first two runs (0.53% in the first run and 0.37% in the second run) was low, while the leaching was negligible in

Table 2. Epoxidation of alkenes with H₂O₂ catalyzed by CFeGO@MnSalBr^a

	Substrate	Product	Time (min)	Conversion (%) ^b	Epoxide selectivity (%)	TOF (h ⁻¹)
1			10	98	100	96.1
2			15	95	92	63.3
3			15	85	90	64.6
4			15	90	91	80
5			15	70	(88% exo) (12% endo)	46.7
6			15	100	93	66.7
6			15	71	100	47.3
8			20	43	100	21.7
9			20	32	100	16.2

^aReaction conditions: Alkene (0.5 mmol), H₂O₂ (5 mmol), catalyst (100 mg, 0.03 mmol), EtOH (4 mL), NaHCO₃ (0.5 mmol). ^bGC yield based on the starting alkene.

Table 3. Comparison of reaction conditions and TOF(h⁻¹) obtained in the presence of CFeGO@MnSalBr with some of the previously reported systems for the epoxidation of cyclooctene, cyclohexene, and styrene

Catalyst	Substrate	Time (h)	Catalyst amount (mmol)	Reaction conditions			TOF (h ⁻¹)	[Ref.]
				Oxidant	Yield (%)			
[Mn ^{III} (salophen)]@imidazole modified magnetite graphene oxide	Cyclooctene	0.17	0.03	H ₂ O ₂	98	96.1	This work	
	Cyclohexene	0.25			87	63.3		
	Styrene	0.25			80	64.6		
[Mn ^{III} (salophen)]@silica-containing triazine dendrimer	Cyclooctene	2.5	0.02	NaIO ₄	95	9.5	[10]	
	Cyclohexene	3			90	7.5		
	Styrene	3			83	6.91		
[Mn ^{III} (salophen)]@Zeolite	Cyclooctene	10	0.45	NaIO ₄	92	2.1	[20]	
	Cyclohexene	10			84	1.91		
	Styrene	10			80	1.98		
[Mn ^{III} (salophen)]@imidazole modified silica	Cyclooctene	3	0.042	NaIO ₄	95	7.38	[19]	
	Cyclohexene	3			93	7.62		
	Styrene	3			86	7.15		
[Mn ^{III} (salophen)]@polystyrene bound imidazole	Cyclooctene	2.5	0.042	NaIO ₄	98	4.67	[15]	
	Cyclohexene	2.5			94	4.70		
	Styrene	2.5			94	4.62		
[Mn ^{III} (salophen)]@1,4-diaminobenzene modified MWCNTs	Cyclooctene	2.5	0.06	NaIO ₄	99	6.60	[13]	
	Cyclohexene	2.5			94	6.47		
	Styrene	3			85	5.06		
[Mn ^{III} (salophen)]@polystyrene bound 1,4-phenylenediamine	Cyclooctene	2.5	0.054	NaIO ₄	98	3.62	[16]	
	Cyclohexene	2.5			91	3.67		
	Styrene	2.5			92	3.55		

the subsequent runs. The FT-IR spectroscopy of the catalyst recovered after use several times showed no change in its IR spectra (Figure 2f), implying the possibility of maintaining CFeGO@MnSalBr after the catalytic activity.

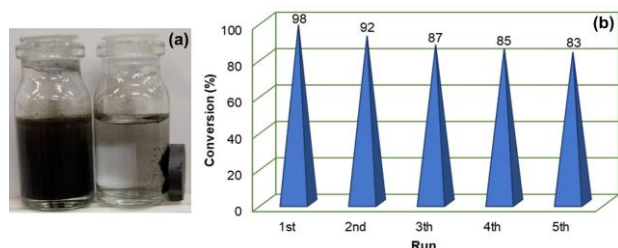


Figure 8. (a) Images recorded during the extraction of the supernatant of the oxidation reaction using the solid CFeGO@MnSalBr in the absence and presence of a magnet, (b) Recyclability of CFeGO@MnSalBr in the oxidation of cyclooctene

4. CONCLUSIONS

In this study, Mn(III) Salophen was successfully synthesized and attached to magnetite graphene oxide (CoFe₂O₄/GO.Im) by a direct covalent bond through imidazole as an axial ligand. This heterogeneous catalyst, CFeGO@MnSalBr, can oxidize a range of olefins, including linear and cyclic ones, into corresponding epoxides under mild conditions in the presence of H₂O₂. It was used as an efficient catalyst in epoxidation and featured as eco-friendly and highly reusable. Besides, it was found to have a short reaction time and was easily separable with a magnet.

CONFLICTS OF INTEREST

The authors have declared that there is no conflict of interest.

ACKNOWLEDGMENTS

We are thankful to the Research Council of Yazd University for their partial support of this research.

AUTHOR INFORMATION

Corresponding Author

Robabeh Hajian: Email: rhajian@yazd.ac.ir,
 ORCID:0000-0002-4637-357X

REFERENCES

- E. J. de Vries, D. B. Janssen, *Curr. Opin. Biotechnol.* **2003**, *14*, 414-420.
- Z. N. Song, J. C. Yuan, Z. P. Cai, D. Lin, X. Feng, N. Sheng, Y. B. Liu, X. B. Chen, X. Jin, D. Chen, C. H. Yang, *Green Energy Environ.* **2020**, *5*, 473-483.
- D. Mohajer, R. Tayebbe, H. Goudarziafshar, *J. Chem. Res., Synop.* **1999**, 168-169.
- S. Y. Liu, D. G. Nocera, *Tetrahedron Lett.* **2006**, *47*, 1923-1926.
- Z. Tang, X. Chen, X. Pang, Y. Yang, X. Zhang, X. Jing, *Biomacromolecules*, **2004**, *5*, 965-970.
- A. Neshat, M. Kakavand, F. Osanlou, P. Mastrorilli, E. Schingaro, E. Mesto, S. Todisco, *Eur. J. Inorg. Chem.* **2020**, 2020, 480-490.
- S. Pakvojoud, M. H. Ardakani, S. Saeednia, E. Heydari-Bafrooei, *J. Sulfur Chem.* **2020**, *41*, 561-580.
- S. R. Pour, A. Abdolmaleki, M. Dinari, *J. Mater. Sci.* **2019**, *54*, 2885-2896.
- M. Suresh, V. Prakash, *E-J. Chem.* **2011**, *8*, 1408-1416.
- M. A. Fardjahromi, M. Moghadam, S. Tangestaninejad, V. Mirkhani, I. Mohammadpoor-Baltork, *RSC Adv.* **2016**, *6*, 20128-20134.
- B. Karami, M. Montazerzohori, M. H. Habibi, *J. Chem. Res.* **2006**, 2006, 490-492.
- C. Sarma, P. K. Chaurasia, S. L. Bharati, *Russ. J. Gen. Chem.* **2019**, *89*, 517-531.
- S. Tangestaninejad, M. Moghadam, V. Mirkhani, I. Mohammadpoor-Baltork, M. S. Saedi, *Appl. Catal., A*, **2010**, *381*, 233-241.
- L. Rouco, A. M. Gonzalez-Noya, R. Pedrido, M. Maneiro, *Antioxidants* **2020**, *9*, 727-755.
- M. Ahmadi, M. Bahadori, V. Mirkhani, M. Moghadam, S. Tangestaninejad, I. Mohammadpoor-Baltork, *Inorg. Chem. Res.* **2020**, *4*, 51-65.
- V. Mirkhani, M. Moghadam, S. Tangestaninejad, B. Bahramian, *Appl. Catal., A*, **2006**, *311*, 43-50.
- R. Hajian, F. Jafari, *J. Iran. Chem. Soc.* **2019**, *16*, 563-570.
- M. A. Fardjahromi, M. Moghadam, S. Tangestaninejad, V. Mirkhani, I. Mohammadpoor-Baltork, *J. Iran. Chem. Soc.* **2017**, *14*, 1317-1323.
- V. Mirkhani, M. Moghadam, S. Tangestaninejad, B. Bahramian, *Appl. Catal., A*, **2006**, *313*, 122-129.
- M. Torke, S. Tangestaninejad, V. Mirkhani, M. Moghadam, I. Mohammadpoor-Baltork, A. R. Khosropour, *J. Inorg. Organomet. Polym. Mater.* **2013**, *23*, 923-929.
- V. Mirkhani, M. Moghadam, S. Tangestaninejad, B. Bahramian, A. Mallekpoor-Shalamzari, *Appl. Catal., A*, **2007**, *321*, 49-57.
- R. Hajian, Z. Alghour, *Chin. Chem. Lett.* **2017**, *28*, 971-975.
- M. Masteri-Farahani, M. Karimi Alavijeh, M. -S. Hosseini, *Inorg. Chem. Res.* **2020**, *4*, 261-269.
- A. Nodzewska, A. Wadolowska, M. Watkinson, *Coord. Chem. Rev.* **2019**, *382*, 181-216.
- L. J. Chen, F. M. Mei, G. X. Li, *React. Kinet. Catal. Lett.* **2009**, *98*, 99-105.
- M. Ghazizadeh, A. Badiei, I. Sheikhshoae, *Arabian J. Chem.* **2017**, *10*, S2491-S2498.

27. V. Mirkhani, M. Moghadam, S. Tangestaninejad, S. Hajibagheri, *J. Iran. Chem. Soc.* **2010**, *7*, 641-645.
28. M. Moghadam, V. Mirkhani, S. Tangestaninejad, I. Mohammadpoor-Baltork, H. Kargar, I. Sheikhsheaei, M. Hatefi, *J. Iran. Chem. Soc.* **2011**, *8*, 1019-1029.
29. T. Dideikin, A. Y. Vul, *Front. Phys.* **2019**, *6*, 149-162.
30. F. Farjadian, S. Abbaspour, M. A. A. Sadatlu, S. Mirkhani, A. Ghasemi, M. Hoseini-Ghahfarokhi, N. Mozaffari, M. Karimi, M. R. Hamblin, *ChemistrySelect*, **2020**, *5*, 10200-10219.
31. S. Shamailla, A. K. L. Sajjad, A. Iqbal, *Chem. Eng. J.* **2016**, *294*, 458-477.
32. M. Baghayeri, M. Ghanei-Motlagh, R. Tayebee, M. Fayazi, F. Narenji, *Anal. Chim. Acta* **2020**, *1099*, 60-67.
33. S. Kumari, A. Shekhar, D. D. Pathak, *RSC Adv.* **2016**, *6*, 15340-15344.
34. S. Rayati, E. Khodaei, S. Shokoohi, M. Jafarian, B. Elmi, A. Wojtczak, *Inorg. Chim. Acta*, **2017**, *466*, 520-528.
35. A. Zarnegaryan, Z. Pahlevanneshan, M. Moghadam, S. Tangestaninejad, V. Mirkhani, I. Mohammadpoor-Baltork, *J. Iran. Chem. Soc.* **2019**, *16*, 747-756.
36. Q. S. Zhao, C. Bai, W. F. Zhang, Y. Li, G. L. Zhang, F. B. Zhang, X. B. Fan, *Ind. Eng. Chem. Res.* **2014**, *53*, 4232-4238.
37. L. Qian, P. Liu, S. Shao, M. J. Wang, X. Zhan, S. X. Gao, *Chem. Eng. J.* **2019**, *360*, 54-63.
38. G. Q. Lv, C. Y. Chen, B. Q. Lu, J. L. Li, Y. X. Yang, C. M. Chen, T. S. Deng, Y. L. Zhu, X. L. Hou, *RSC Adv.* **2016**, *6*, 101277-101282.
39. S. Verma, M. Aila, S. Kaul, S. L. Jain, *RSC Adv.* **2014**, *4*, 30598-30604.
40. H. L. Su, S. J. Wu, Z. F. Li, Q. S. Huo, J. Q. Guan, Q. B. Kan, *Appl. Organomet. Chem.* **2015**, *29*, 462-467.
41. M. Bagherzadeh, H. Karimi, M. Amini, *J. Coord. Chem.* **2017**, *70*, 2986-2998.
42. A. Allahresani, *Iran. Chem. Commun.* **2018**, *6*, 180-191.
43. S. S. Wu, D. H. Lan, N. A. Y. Tan, R. Wang, C. T. Au, B. Yi, *J. Chem. Soc. Pak.* **2021**, *43*, 57-66.
44. B. Vangroenou, P. F. Bongers, A. L. Stuyts, *Mater. Sci. Eng.* **1969**, *3*, 317-392.
45. S. P. Dalawai, S. Kumar, M. A. S. Aly, M. Z. H. Khan, R. M. Xing, P. N. Vasambekar, S. H. Liu, *J. Mater. Sci.: Mater. Electron.* **2019**, *30*, 7752-7779.
46. K. K. Kefeni, B. B. Mamba, *Sustainable Mater. Technol.* **2020**, *23*, 140-158.
47. S. Y. Srinivasan, K. M. Paknikar, D. Bodas, V. Gajbhiye, *Nanomedicine* **2018**, *13*, 1221-1238.
48. B. Maleki, F. Taheri, R. Tayebee, F. Adibian, *Org. Prep. Proced. Int.* **2021**, *53*, 284-290.
49. Z. Song, W. Ran, F. Wei, *Water Sci. Technol.* **2017**, *75*, 397-405.
50. S. Y. Zhao, D. -G. Lee, C. -W. Kim, H. -G. Cha, Y. -H. Kim, Y. -S. Kang, *Bull. Korean Chem. Soc.* **2006**, *27*, 237-242.
51. M. Kooti, M. Afshari, *Catal. Lett.* **2012**, *142*, 319-325.
52. A. Saffar-Teluri, *RSC Adv.* **2015**, *5*, 70577-70585.
53. Q. F. Zhou, Z. J. Wan, X. F. Yuan, J. Luo, *Appl. Organomet. Chem.* **2016**, *30*, 215-220.
54. L. W. Chen, D. H. Ding, C. Liu, H. Cai, Y. Qu, S. J. Yang, Y. Gao, T. M. Cai, *Chem. Eng. J.* **2018**, *334*, 273-284.
55. R. Tabit, O. Amadine, Y. Essamlali, K. Danoun, A. Rhihil, M. Zahouily, *RSC Adv.* **2018**, *8*, 1351-1360.
56. V. Abbasi, H. Hosseini-Monfared, S. M. Hosseini, *New J. Chem.* **2017**, *41*, 9866-9874.
57. V. Abbasi, H. Hosseini-Monfared, S. M. Hosseini, *Appl. Organomet. Chem.* **2017**, *31*, 10.
58. R. Hajian, A. Ehsanikhah, *Chem. Phys. Lett.* **2018**, *691*, 146-154.
59. R. Hajian, S. Tangestaninejad, M. Moghadam, V. Mirkhani, A. R. Khosropour, *Comptes Rendus Chimie* **2012**, *15*, 975-979.
60. R. Hajian, S. Tangestaninejad, M. Moghadam, V. Mirkhani, I. Mohammadpoor-Baltork, *J. Iran. Chem. Soc.* **2016**, *13*, 1061-1067.
61. R. Hajian, S. Tangestaninejad, M. Moghadam, V. Mirkhani, I. Mohammadpoor-Baltork, A. R. Khosropour, *J. Coord. Chem.* **2011**, *64*, 4134-4144.
62. S. Tangestaninejad, M. Moghadam, V. Mirkhani, I. Mohammadpoor-Baltork, R. Hajian, *Inorg. Chem. Commun.* **2010**, *13*, 1501-1503.
63. R. Tayebee, *J. Chem. Sci.* **2006**, *118*, 429-433.
64. H. Jacobsen, L. Cavallo, *Organometallics* **2006**, *25*, 177-183.
65. D. C. Marcano, D. V. Kosynkin, J. M. Berlin, A. Sinitskii, Z. Sun, A. Slesarev, L. B. Alemany, W. Lu, J. M. Tour, *ACS Nano* **2010**, *4*, 4806-4814.
66. K. Maaz, A. Mumtaz, S. Hasanain, A. Ceylan, *J. Magn. Magn. Mater.* **2007**, *308*, 289-295.
67. D. Chen, A. Martell, *Inorg. Chem.* **1987**, *26*, 1026-1030.
68. S. Rana, J. Philip, B. Raj, *Mater. Chem. Phys.* **2010**, *124*, 264-269.
69. J. Parhizkar, M. H. Habibi, *J. Water Environ. Nanotechnol.* **2019**, *4*, 17-30.
70. M. Garcia, V. Moreno, S. X. Delgado, A. E. Ramirez, L. A. Vargas, M. A. Vicente, A. Gil, L. A. Galeano, *J. Mol. Catal. A: Chem.* **2016**, *416*, 10-19.
71. S. Lane, M. Vogt, V. J. DeRose, K. Burgess, *J. Am. Chem. Soc.* **2002**, *124*, 11946-11954.